THE JOURNAL OF PHYSICAL CHEMISTRY C

Article

pubs.acs.org/JPCC

Charge Compensation in Sodium Borophosphate Glasses Studied by $^{11}B\{^{23}Na\}$ and $^{31}P\{^{23}Na\}$ Rotational Echo Double Resonance Spectroscopy

Lena Marie Funke[†] and Hellmut Eckert*[,†,‡]

[†]Institut für Physikalische Chemie, Westfälische Wilhelms-Universität Münster, Corrensstraße 30, D 48149 Münster, Germany

[‡]Instituto de Física em São Carlos, Universidade de São Paulo, CEP 369, São Carlos 13560-590, Brazil

Supporting Information

ABSTRACT: Network former−network modifier interactions in three sodium borophosphate glasses have been probed by $^{11}B\{^{23}Na\}$ and $^{31}P\{^{23}Na\}$ rotational echo double resonance (REDOR) experiments. For the compositions chosen essentially all of the boron atoms in these glasses are four-coordinated and, thus, of formally anionic character, whereas the majority of the phosphorus species are of the (nominally charge-neutral) $P^{(3)}$ type. Despite this fact, the dipolar second moments $M_2(^{11}B\{^{23}Na\})$ and $M_2(^{31}P\{^{23}Na\})$ extracted from these REDOR data indicate that the sodium cations interact significantly more strongly with the phosphate than with the borate species. As a matter of fact, the distance sums $\sum r_{P-Na}^{-6}$ calculated from these second moments are close to those measured in sodium ultraphosphate glasses with similar sodium concentrations, whereas the corresponding $\sum r_{B-Na}^{-6}$ values are significantly smaller than those measured in sodium borate glasses with comparable sodium concentrations. These results are corroborated by complementary $^{23}Na\{^{31}P\}$ and $^{23}Na\{^{11}B\}$ REDOR experiments. As supported by bond valence arguments, the formation of $P^{(3)}$−O−$B^{(4)}$ linkages in borophosphate glasses results in a charge displacement away from the four-coordinated boron atoms toward the nonbridging oxygen atoms on the $P^{(3)}$ units. These charge dispersal effects result in shallower Coulomb traps, thereby facilitating ionic mobility.

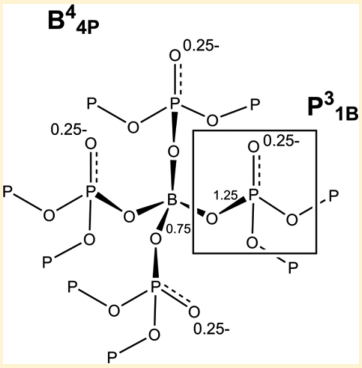

INTRODUCTION

Alkali borophosphate glasses of composition $(M_2O)_y[(P_2O_5)_{1-x}(B_2O_3)_x]_{1-y}$ (M = Li−Cs; $0.3 < y \leq 0.5$; $0 < x < 1.0$) are known for their strongly positive mixed-network former effect upon their ionic conductivities. In particular, glasses with relatively low boron contents show both much higher thermal and mechanical stability and also higher ionic conductivities than expected from an interpolation of the respective values of the single-network former end members.[1−4] Detailed solid state NMR work has shown that the increased thermal and mechanical stability can be attributed to the dominant presence of four-coordinate boron in these glasses, resulting in an overall increase in bond connectivity.[5−9] The concomitant increase in the ionic mobility is more difficult to explain and must be discussed on the basis of the local environment of the cationic species. We previously proposed that the positive mixed network former effect on the electrical conductivity of alkali borophosphate glasses arises from a higher degree of charge dispersal within the anionic network when compared to pure phosphate glasses.[9] In this connection, detailed $^{11}B/^{31}P$ double resonance results showed that alkali borophosphate glasses present a strong preference for the formation of heteroatomic P−O−B over homoatomic P−O−P and B−O−B linkages.[9−14] These results have been confirmed by theoretical analyses using statistical mechanics and molecular dynamics simulation approaches.[15−17] The local structural units in the network can be described according to the $P^{(n)}{}_{mB}$ and $B^{(n)}{}_{mP}$ notations where n describes the number of bridging oxygen atoms per polyhedron and m is the number of oxygen atoms forming heteroatomic P−O−B bridges in which the structural unit is involved.[9] Thus, at low borate concentration the dominant B species are found to be $B^{(4)}{}_{4P}$ units, which are predominantly bonded to (formally neutral) $P^{(3)}$ species. As proposed in ref 9, such $B^{(4)}{}_{4P}$ species should not be considered anionic as the bond valence of the four-coordinate boron atom (0.75) and the bond valence of the four-coordinate phosphorus atoms (1.25) compensate each other, resulting in perfectly charge-balanced oxygen atoms within the P−O−B bridges. We suggested that as a result the negative charge (formally located at the $B^{(4)}$ center) is actually partially shifted toward the nonbridging oxygen atoms of the $P^{(3)}$ units linked to it bestowing some anionic character to these species (see Figure 1). The resulting charge dispersal creates rather shallow Coulomb traps for the mobile alkali ions, held responsible for the enhanced ionic conductivities (and reduced ion jump activation energies) of these glasses. Similar charge delocalization mechanisms can be found for other borophosphate compositions. If this model is indeed applicable, it would be

Received: November 27, 2015
Revised: January 20, 2016
Published: January 20, 2016

DOI: 10.1021/acs.jpcc.5b11608
J. Phys. Chem. C 2016, 120, 3196−3205

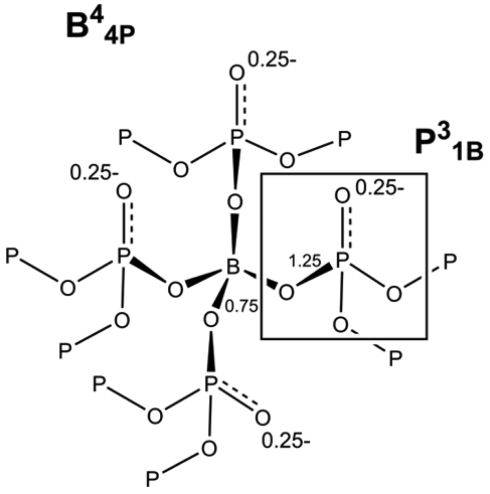

Figure 1. Charge distribution of the structural units $B^{(4)}_{4P}$ and $P^{(3)}_{1B}$ in alkali borophosphate glasses according to bond valence considerations. The implied nonsymmetrical electron distributions are illustrated by the conical shape of the B−O and P−O bonds.

expected that the mobile ions in these glasses interact more strongly with the $P^{(3)}$ units than with the $B^{(4)}$ units. In other words, the above scenario predicts overall closer P−Na than B−Na distances. This issue can be addressed by advanced dipolar solid state NMR methods that can measure heteronuclear magnetic dipolar coupling strengths in an element-selective and even site-selective fashion. In the general case, a nucleus *S*, whose signal is being observed in the NMR experiment, is surrounded by numerous heteronuclei *I* at various distances r_{IS}, which generate a local dipolar field at the site of the *S* nuclei. This local field can be quantified in terms of a dipolar second moment, $M_{2I\text{-}S}$, which can be calculated from the internuclear distances according to the well-known van Vleck equation:[18]

$$M_{2I\text{-}S} = \frac{4}{15}\left(\frac{\mu_o}{4\pi}\right)^2 I(I+1)\gamma_I^{\,2}\gamma_S^{\,2}\hbar^2 \sum_I r_{IS}^{\,-6} \quad (1)$$

In expression 1, γ_S is the gyromagnetic ratio of the observe nuclei *S* while *I* and γ_I are the nuclear spin quantum number and the gyromagnetic ratio of these heteronuclei, and all the other symbols have their usual meanings.

In the present contribution we will compare ^{31}P−^{23}Na versus ^{11}B−^{23}Na magnetic dipole−dipole coupling strengths, using the rotational echo double resonance method.[19] Results are presented for three sodium borophosphate glass compositions, in which connectivities such as those shown in Figure 1 are expected to occur. On the basis of the quantitative analysis of these interactions, we conclude that it is indeed the phosphate species which are mainly responsible for charge compensation in these glasses.

EXPERIMENTAL SECTION

Sample Preparation and Characterization. Table 1 summarizes the compositions and physical properties of the glasses under investigation. The starting materials, anhydrous Na_2CO_3 (Acros, 99.9%) and $NH_4H_2PO_4$ (Acros, 99.9%), were predried for 48 h at 120 °C. B_2O_3 (Acros, 99%) was heated for 2 h at 900 °C in a platinum crucible and quenched to form a glass. It was immediately stored in an argon-filled box and ground prior to glass preparation. 1−12 g batches of the

Table 1. Glass Compositions and Glass Transition Temperatures, T_g, Obtained in the Present Study[a]

sample	composition Na_2O:B_2O_3:P_2O_5	mol % Na_2O	mol % B_2O_3	mol % P_2O_5	$T_g \pm 5$ (K)
A	0.8:1.0:4.2	13.3	16.7	70.0	593
B	1.0:1.0:2.0	25.0	25.0	50.0	695
C	1.0:0.5:1.5	33.3	16.7	50.0	640
D	1.0:2.0:0.0	33.3	66.7		744

[a]A and B are new compositions, C corresponds to a glass previously studied in ref 9, and D is $Na_2B_4O_7$ glass.

mixtures (see Table 2) were degassed and melted in a platinum crucible inside a Thermoconcept muffle furnace at 1000−1200 °C. The appropriate temperatures for the formation of homogeneous melts were determined in advance to limit the melting time at high temperatures to 15 min and minimize evaporation losses. Melts were quenched by placing the crucible onto a copper plate held at room temperature. As some compositions formed highly viscous glass melts, this cooling procedure was preferred over melt quenching via pouring. To limit exposure to ambient moisture and ensure sample quality over a long period of time, glass samples were stored in an argon-filled glovebox. All the glasses were found to be homogeneous and transparent upon visual inspection, and DSC showed no evidence of phase separation. For samples B−D, excess mass losses were less than or equal to 2%. Glass A, having the batch composition $Na_2O{\cdot}B_2O_3{\cdot}4P_2O_5$, forms clear melts only at 1200 °C. Excess mass losses around 10% were encountered in this case, despite the short melting times of 15 min used. The exact composition of this material was determined by inductively coupled plasma atomic emission spectroscopy (ICP-AES) with aqua regia digestion. To determine the boron content, the glass was chemically dissolved with microwave-assisted HF−HNO_3−HCl digestion according to DIN EN ISO 11885 and analyzed with ICP-AES.

Table 2. Measurement Conditions for the Double Resonance Experiments Conducted in the Present Study

			π-pulse length (μs)	
experiment	B_0 (T)	ν_r (kHz)	observe nucleus	nonobserve nucleus
^{11}B{^{31}P}REDOR	7.05	13.0	14.0	9.7
^{11}B{^{23}Na} REDOR	11.7	12.0	7.9[a]/4.8[b]	17.5
^{23}Na{^{11}B} REDOR	11.7	12.0	17.5	7.9[a]/4.8[b]
^{31}P{^{23}Na} REDOR	9.4	14.0	10.3	5.7
^{23}Na{^{31}P} REDOR	9.4	14.0	5.7	10.3

[a]For four-coordinate boron. [b]For three-coordinate boron.

Thermal analyses were carried out with a Netzsch DSC Phönix differential scanning calorimeter using a heating rate of 10 K min^{-1}. Using the Proteus Thermal Analysis software, the glass transition temperatures were determined from the onset region of the observed thermal event by the tangent intersection method. A LabRAM HR Raman microscope spectrometer from Jobin Yvon Horiba was used to collect the Raman spectra from smooth sample regions. The spectra were taken using a 532 nm laser focused with a 50× objective, a 1800 lines/mm grating, and a CCD detector operated at an acquisition time of 10 s. 50−100 scans were averaged to enhance the signal-to-noise ratio.

DOI: 10.1021/acs.jpcc.5b11608
J. Phys. Chem. C 2016, 120, 3196−3205

Solid State NMR. All experiments were conducted at room temperature on a Bruker-Avance-III 300 MHz spectrometer, a Bruker-Avance-DSX-400 spectrometer, and a Bruker-Avance-DSX-500 spectrometer, equipped with fast MAS capabilities. To minimize radio-frequency amplitude inhomogeneities, all the REDOR experiments were conducted with rotors that were only filled in the middle 1/3 of their total volumes. The ^{11}B-MAS NMR spectra were recorded at 7.05 and 11.7 T in 4 mm MAS probes operated at a spinning frequency of ν_r = 12.0 kHz, and pulse lengths of 1.0 μs were used (22.5° flip angle). To ensure complete relaxation, signal averaging required recycle delays of 5−30 s. The ^{31}P-MAS NMR spectra were recorded at 7.1 T using a 2.5 mm MAS probe operated at a spinning frequency 28.0 kHz. ^{23}Na single pulse experiments were conducted at 11.7 T, using a 4 mm MAS probe operated at 14.0 kHz. Short excitation pulses of 1.0 μs were used, and recycle delays were set to 0.5−1 s. ^{23}Na z-filtered TQMAS-NMR experiments[20] were performed at 9.4 and 11.7 T and MAS rotation frequencies of 14.0 kHz. Typical pulse lengths for the first hard pulse were 4.3−7.6 μs. The second hard pulse was 1.3−2.1 μs long, and the length of the soft detection pulse was 10 μs. Repetition times were set to 0.5−1 s. The isotropic chemical shift δ_{iso} and the second-order quadrupolar effect (SOQE) were calculated from the centers of gravity in the F1 and F2 dimensions of the TQMAS spectra as previously described.[21] The Fourier transformed phased signals were analyzed using the Dmfit 2011 program package.[22] The specific measurement conditions selected for the various heteronuclear X−Y double resonance experiments are summarized in Table 2. They were conducted with a saturation comb ensuring reproducible initial conditions. Sodium pyrophosphate ($Na_4P_2O_7$) and sodium borophosphate ($Na_5B_2P_3O_{13}$)[23] were used as reference and calibration materials. All the REDOR experiments used the standard REDOR sequence of Gullion and Schaefer,[19] using XY-4 phase cycles[24] on the recoupling π-pulses.

To extract dipolar coupling information from these experiments, an approximation is used, according to which the normalized REDOR difference signal follows a parabolic dependence on evolution time according to $\Delta S/S_0 \sim (NT_r)^2$ within the initial region defined by the condition $\Delta S/S_0 \leq 0.2$.[25] For REDOR experiments involving quadrupolar nuclei one has to take into consideration the different Zeeman states of the dephaser nuclei as well as the fact that in the case of strong quadrupolar interactions the dephaser nuclei in the noncentral Zeeman states contribute very little to the REDOR effect, because of the large shifts in resonance frequencies caused by first-order quadrupolar perturbations. A complete analysis of REDOR experiments involving quadrupolar dephaser nuclei with spin 3/2 has been previously presented.[26] Alternatively, we use here a more practical approach, based on the approximate formula[27]

$$\frac{\Delta S}{S_0} = \frac{1}{I(I+1)\pi^2}(NT_R)^2 f M_2(S\{I\}) \quad (2)$$

previously proposed, where all the complications generated by the quadrupolar nature of the dephaser nuclei as well as further experimental imperfections (finite pulse length and off-resonance effects) are taken into consideration by a calibration factor f, which is measured on a crystalline model compound featuring similar spin dynamics as the sample under study. For REDOR experiments involving quadrupolar ^{23}Na and ^{11}B nuclei, the value of f defined in this manner usually lies within the range 0.05−0.2, as the $|\pm 1/2\rangle \leftrightarrow |\pm 3/2\rangle$ satellite transitions of the spin-3/2 nuclei are affected by large off-resonance shifts owing to first-order quadrupolar perturbation effects. This renders the π recoupling pulses applied to these nuclei much less efficient. For appropriate calibration, it is important that the crystalline model compound features comparable nuclear electric quadrupolar interaction strengths as those found in the glasses. A suitable model compound is the crystalline sodium borophosphate $Na_5B_2P_3O_{13}$ whose NMR spectroscopic features have been previously characterized in detail.[28] It features $B^{(4)}_{3P}$ and $P^{(2)}_{2B}$ units linked by P−O−B connectivities with P−B distances between 265 and 277 pm, and the B···Na and P···Na distances are similar to those expected in the present glasses.

RESULTS AND DISCUSSION

Raman Spectroscopy. Figure 2 shows the Raman spectra of the glasses under study. All three borophosphate glasses

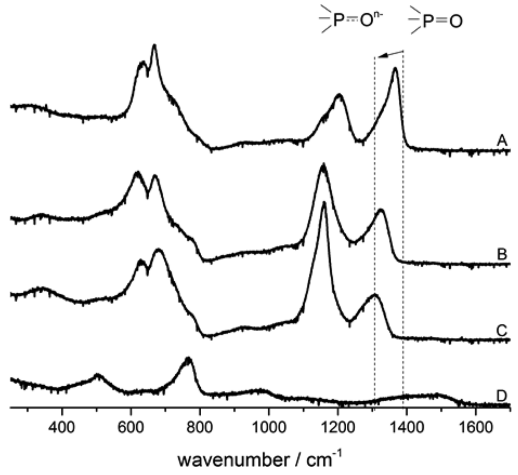

Figure 2. Raman spectra of the investigated borophosphate and borate glasses with parallel lines drawn at 1310 cm^{-1} (scattering wavenumber observed for glass C) and at the vibrational wavenumber of $P^{(3)}$ in phosphorus pentoxide (1390 cm^{-1}).

show characteristic bands near 670, 1160, and 1350 cm^{-1} which can be assigned to the symmetric P−O−P vibration, the symmetric PO_2 stretching vibration in metaphosphate ($P^{(2)}$) units, and the P═O vibration of $P^{(3)}$ groups, respectively. The P═O vibration band is shifted to lower frequencies with increasing Na_2O content, indicating a successive weakening of the P═O double bonds. Consistent with the previous interpretation of similar band shifts in alkali ultraphosphate glasses,[29] this effect can be attributed to interactions between the $P^{(3)}$ units and nearby alkali ions, indicating that these nonbridging oxygen atoms are part of the first coordination sphere of the sodium ions. The observed shifts to lower frequencies have also been observed in other borophosphate glasses and interpreted along the same lines.[9] This interpretation is also substantiated by the cation effect: the wavenumber of the P═O stretching mode that is observed for the sample C is in between those measured in ref 9 for the homologous lithium and potassium borophosphate glasses. Comparing the wavenumbers of this vibrational mode among samples A (1370 cm^{-1}), B (1330 cm^{-1}), and C (1310 cm^{-1}), we further note that the shift of the Raman band toward lower

DOI: 10.1021/acs.jpcc.5b11608
J. Phys. Chem. C 2016, 120, 3196−3205

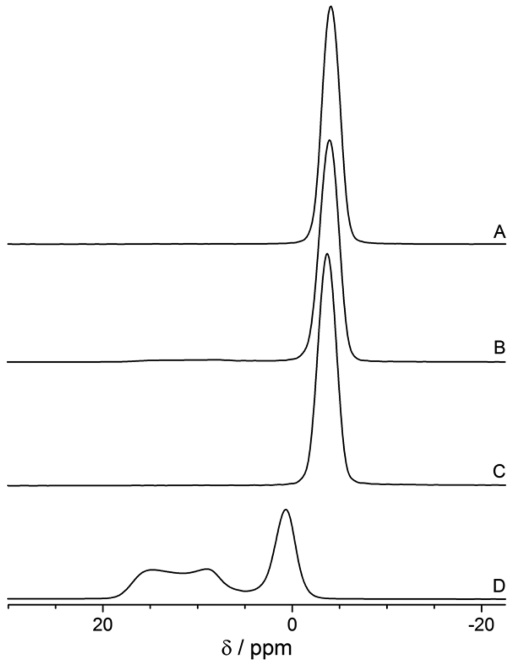

Figure 3. ^{11}B MAS NMR spectra of the investigated glass system, spinning frequency ν_r = 12.0 kHz, B_0 = 11.7 T.

frequencies is correlated with the Na content, reflecting the increasing strength of the interaction of the $P^{(3)}$ units with the sodium ions. The scattering peak at 1160 cm^{-1} can be attributed to $P^{(2)}$ units which undoubtedly contribute to the structure of all three glasses, confirming the conclusion from solid state NMR (see subsequent section). Finally, the binary sodium diborate glass D shows a Raman spectrum that is in good agreement with the literature.[30−33] The bands at 500 and 760 cm^{-1} can be assigned to the breathing vibration of rings containing BO_3 and BO_4 units within pentaborate, tetraborate, and diborate groups. Both of these signals are absent in the borophosphate glasses A−C giving no evidence for such ring structures in them. This result, taken together with the NMR data to be discussed below, suggests that the number of B−O−B bonds in these glasses is low. The band at 1450 cm^{-1} in sample D is assigned to the stretching mode of nonbridging oxygen atoms attached to three-coordinate boron species. Such metaborate ($B^{(2)}$) units are well-known to occur in binary sodium borate glasses containing more than 30 mol % Na_2O. In contrast, our Raman spectra give no evidence for any $B^{(2)}$ groups in the samples A−C.

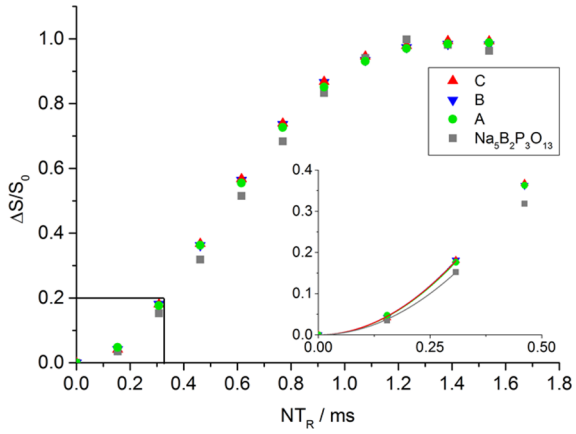

Figure 4. ^{11}B{^{31}P} REDOR results on the glasses and the model compound $Na_5B_2P_3O_{13}$, spinning frequency ν_r = 13.0 kHz, B_0 = 9.4 T. Measurement errors are represented by symbol sizes. The inset shows a parabolic fit of the data within the initial data range $\Delta S/S_0 < 0.2$.

Table 4. ^{31}P MAS-NMR Spectral Deconvolution, Peak Assignments, and Fitting Parameters

sample	$P^{(n)}{}_{mB}$	δ_{iso} ±10% (ppm)	line width (ppm)	area fraction ± 2 (%)
A	$P^{(3)}{}_{0B}$	−44.0	11.8	29
	$P^{(3)}{}_{1B}$	−36.7	11.3	54
	$P^{(3)}{}_{2B}$	−27.8	8.7	17
B	$P^{(3)}{}_{0B}$	−43.7	13.3	3
	$P^{(3)}{}_{1B}$	−36.3	13.3	23
	$P^{(3)}{}_{2B}$, $P^{(2)}{}_{0B}$	−27.2	13.3	72
	$P^{(3)}{}_{3B}$, $P^{(2)}{}_{1B}$	−14.7	7.9	2
C	$P^{(3)}{}_{0B}$	−42.6	13.0	2
	$P^{(3)}{}_{1B}$	−32.1	12.6	29
	$P^{(2)}{}_{0B}$	−29.6	7.2	8
	$P^{(3)}{}_{2B}$	−24.2	7.9	31
	$P^{(2)}{}_{1B}$	−20.2	8.6	19
	$P^{(3)}{}_{3B}$	−15.7	7.8	7
	$P^{(2)}{}_{2B}$	−12.2	7.5	3

^{11}B and ^{31}P MAS NMR and ^{11}B{^{31}P} REDOR. The 3-fold and 4-fold coordinated boron atoms are exposed to electric field gradients of different symmetry and magnitude and can be well-resolved by ^{11}B MAS NMR. Figure 3 and Table 3 summarize the experimental spectra and their deconvolutions. Consistent with the expectations based on previous studies, the borophosphate glasses show almost exclusively or exclusively four-coordinated boron. Only in sample B a small concentration of three-coordinated boron is detected. On the basis of

Table 3. Deconvolution of the ^{11}B MAS-NMR Spectra, ^{11}B Line-Shape Parameters, and $M_2(^{11}B\{^{31}P\})$ Values Measured for the Borophosphate and Borate Glasses under Study and for $Na_5B_2P_3O_{13}$

sample	$B^{(n)}$	δ_{iso} ± 0.5 (ppm)	line width (ppm)	C_Q ± 0.1 (MHz)	η_Q ± 0.1	area fraction ±2 (%)	$M_2 \times 10^{-6}$ ± 10% (rad^2 s^{-2})
A	$B^{(4)}$	−4.4	2.3			100	18.9
B	$B^{(4)}(1)$	−4.0	2.3			93	19.3
	$B^{(4)}(2)$	−1.4	3.1			2	
	$B^{(3)}$	17.2		2.6	0.6	5	
C	$B^{(4)}$	−3.6	2.2			100	19.2
D	$B^{(4)}$	0.7	2.5			40	
	$B^{(3)}$	18.5		2.6	0.2	50	
	$B^{(2)}$	14.0		2.5	0.5	10	
$Na_5B_2P_3O_{13}$		0.5, −0.1		0.6	0.1		16.2

DOI: 10.1021/acs.jpcc.5b11608
J. Phys. Chem. C 2016, 120, 3196−3205

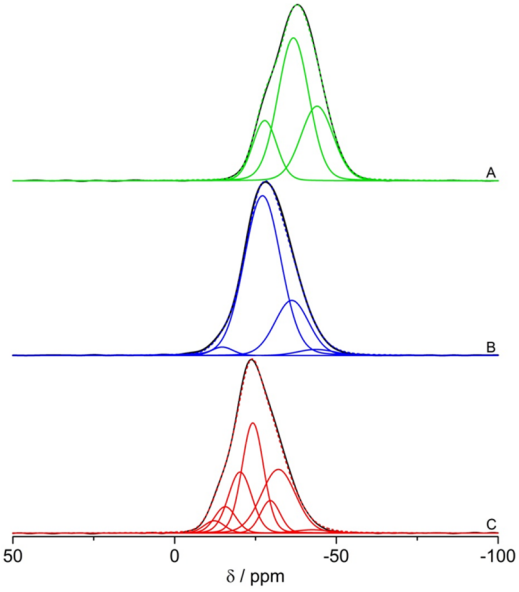

Figure 5. ^{31}P MAS NMR spectra, spinning frequency ν_r = 28.0 kHz, B_0 = 9.4 T. Fits consider mass and charge balances. For glass C, the previously reported fitting approach was used.[9]

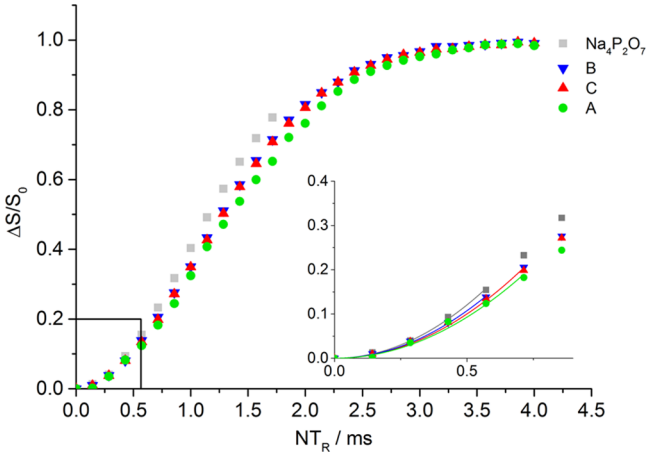

Figure 6. ^{23}Na{^{31}P} REDOR results at a spinning frequency ν_r = 14.0 kHz and B_0 = 11.7 T. Measurement errors are represented by symbol sizes. The inset shows parabolic fits (solid curves) conducted within the data range $\Delta S/S_0 \leq 0.2$.

previous chemical shift correlations in borophosphate glasses with the number of P atoms in the second coordination sphere,[7,9] we can conclude that the number of B−O−P linkages per boron atom is close to four, again consistent with no B−O−B linkages. This is also confirmed by the second moment values $M_2(^{11}B\{^{31}P\})$ measured by REDOR. For the model compound $Na_5B_2P_3O_{13}$, the experimentally observed value of 11.9×10^6 rad^2 s^{-2} in Figure 4 is close to the value of 16.2×10^6 rad^2 s^{-2} expected from the crystal structure, resulting in a calibration factor of 0.73. The M_2 values listed for the glasses in Table 4 already include this correction factor. They are consistently higher than that of the model compound $Na_5B_2P_3O_{13}$, whose crystal structure presents three B−O−P linkages. This result suggests that the boron environment in these glasses is dominated by $B^{(4)}_{4P}$ units.

The ^{31}P MAS NMR spectra and their deconvolutions are summarized in Figures 5 and Table 4. They are rather complex owing to the large number of possible $P^{(n)}_{mB}$ units whose resonances strongly overlap in the spectra. The peak deconvolutions are based on the previous fitting approach discussed in detail in ref 9. The structure of glass A is clearly dominated by $P^{(3)}$ units, with various different degrees of B−O−P connectivity. Glasses B and C show also some contributions from $P^{(2)}$ units, whose signals overlap with those from $P^{(3)}_{1B}$ and $P^{(3)}_{2B}$ groups.

^{23}Na TQMAS-NMR and ^{23}Na{^{31}P} and ^{23}Na{^{11}B} REDOR. ^{23}Na TQ-MAS NMR spectra of the investigated glass samples (data not shown) give no indications of the presence of more than one distinct site. Table 5 summarizes the isotropic chemical shifts δ_{iso}^{cs} and second-order quadrupolar effect (SOQE) values extracted from these data. The observed increase of δ_{iso}^{cs} with increasing Na content (see Table 5) is consistent with other data measured on sodium borate and sodium phosphate glasses.[34,35] In contrast, the SOQE values for borophosphate glasses are within the data range 0.9−1.0 ± 0.1 MHz and differ remarkably from those measured in sodium diborate glass whose chemical shift and SOQE are in good agreement with the literature.[33] The SOQE values of the borophosphate glasses also are significantly lower than those measured for sodium ultraphosphate glasses,[35] suggesting a new type of environment that is unique for borophosphate glasses. Further information regarding the coordination environment of the sodium ions is available from ^{23}Na{^{31}P} and ^{23}Na{^{11}B} REDOR experiments. Figure 6 shows the ^{23}Na{^{31}P} REDOR results obtained on the glasses and the model compound $Na_4P_2O_7$. The second moment values, extracted from these

Table 5. ^{23}Na Isotropic Chemical Shifts and SOQE Values Extracted from TQMAS NMR, Dipolar Second Moments (±10%) Characterizing the Heteronuclear Magnetic Dipolar Coupling Strengths of the ^{23}Na Observe Nuclei with ^{31}P and ^{11}B for the Glasses under Study and the Crystalline Model Compounds Investigated, and Values of $\sum r_{Na-P}^{-6}$ and $\sum r_{Na-B}^{-6}$ (±10%) Calculated from These M_2 Values via Eq 1

sample	δ_{iso}^{cs} ± 0.5 (ppm)	SOQE ± 0.1 (MHz)	$M_2(^{23}Na\{^{31}P\})$ (10^6 rad^2 s^{-2})	$\sum r_{Na-P}^{-6}$ (10^{60} m^{-6})	$M_2(^{23}Na\{^{11}B\})$ (10^6 rad^2 s^{-2})	$\sum r_{Na-B}^{-6}$ (10^{60} m^{-6})
A	−10.1	0.9	4.0	0.0031	6.1	0.0009
B	−9.4	0.9	4.6	0.0035	14.5	0.0022
C	−7.2	1.0	4.3	0.0033	9.3	0.0014
D	−3.3	1.8			36.8 (7.9 μs[a])	0.0056
					49.8 (4.8 μs[b])	0.0076
$Na_4P_2O_7$			5.2	0.0040		
$Na_5B_2P_3O_{13}$					7.1	0.0011.

[a]Dipolar recoupling with π pulse length (parentheses) optimized for four-coordinated boron sites. [b]Dipolar recoupling with π pulse length (parentheses) optimized for three-coordinated boron sites.

DOI: 10.1021/acs.jpcc.5b11608
J. Phys. Chem. C 2016, 120, 3196−3205

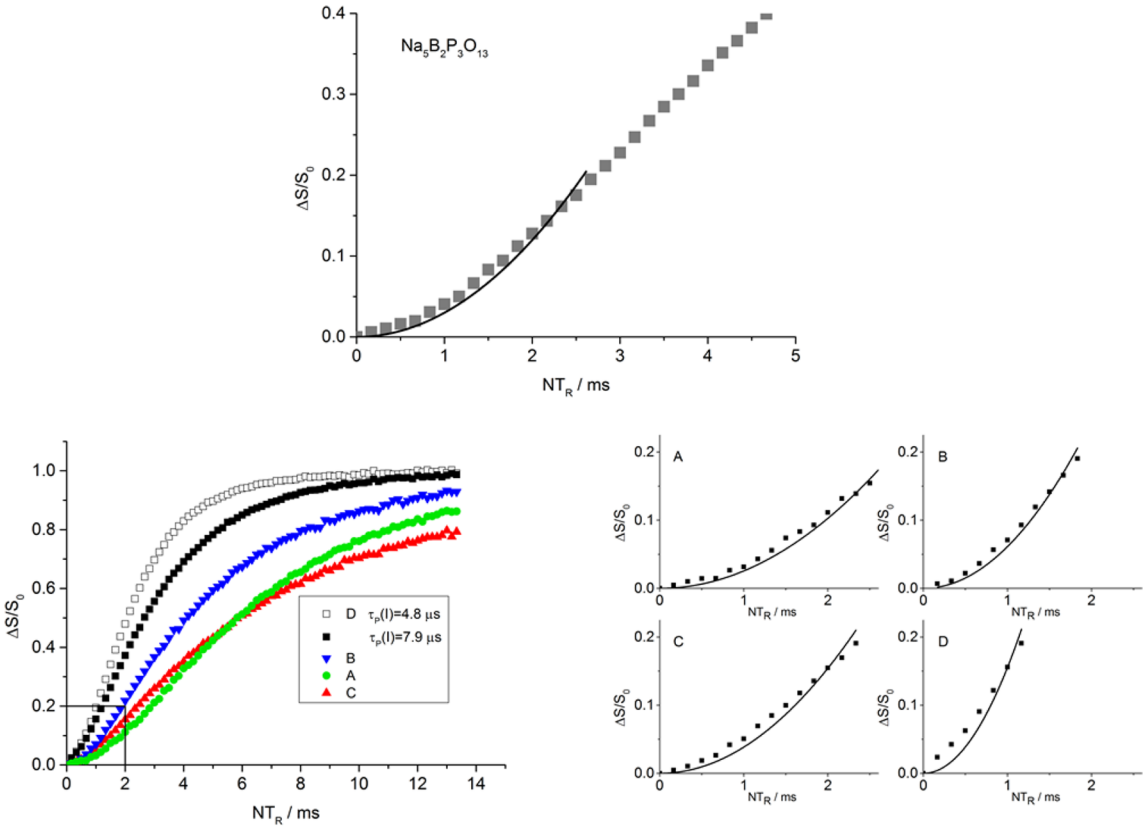

Figure 7. Top: ^{23}Na{^{11}B} REDOR results on $Na_5B_2P_3O_{13}$, including a parabolic fit. Measurement errors are represented by symbol sizes. Bottom: ^{23}Na{^{11}B} REDOR results on the glasses of the present study. Measurement errors are represented by symbol sizes. The corresponding parabolic fits to the latter REDOR curves are shown on the right. Measurements were conducted at a spinning frequency of ν_r = 12.0 kHz and at B_0 = 11.7 T. For the borate glass (D) different π pulse lengths were used in the REDOR experiments reflecting different nutation frequencies of 3-fold and 4-fold coordinated boron.

plots from the initial REDOR curvatures via eq 2, are listed in Table 5. For $Na_4P_2O_7$ the experimentally measured value of 3.6 × 10^6 rad^2 s^{-2} is close to the theoretical value of 5.2 × 10^6 rad^2 s^{-2} expected from eq 1, using the P···Na distances within a distance range of 1360 pm (f = 0.70). The corrected experimental values obtained for the glasses are listed in Table 5. They are similar to those of the model compounds $Na_4P_2O_7$ and $Na_5B_2P_3O_{13}$ as well as a series of $(Na_2O)_x(P_2O_5)_{1-x}$ glasses ($x \leq 0.5$). For a random distribution of borate and phosphate ligands around the sodium species, one would have expected a reduction in $M_2(^{23}Na\{^{31}P\})$ based on the statistical factor, particularly in glass B, where the borate to phosphate ratio is 1:2. There is, however, no clear evidence for such a diminution effect. Thus, the ^{23}Na{^{31}P} REDOR data of the present study consistently suggest that the second coordination sphere of the sodium ions is dominated by phosphate species.

Figure 7 shows corresponding ^{23}Na{^{11}B} REDOR results. The quantification of these experimental data in terms of second moment values is expected to be less accurate as the REDOR curves in the initial data range deviate substantially from parabolic behavior, for both the glasses and the crystalline model compound $Na_5B_2P_3O_{13}$. Nevertheless, the model compound data were used to deduce a calibration factor of 0.16, which was then applied to obtain the corrected $M_2(^{23}Na\{^{11}B\})$ values for the three glasses, listed in Table 5. For $Na_2B_4O_7$ glass, the large difference in quadrupolar coupling constants for $B^{(3)}$ and $B^{(4)}$ results in rather different π pulse lengths for ^{11}B spin inversion. Thus, Table 5 includes two $M_2(^{23}Na\{^{11}B\})$ values, based on optimized π pulse lengths for $B^{(3)}$ and $B^{(4)}$ units, respectively. Both values must be considered underestimates of the true $M_2(^{23}Na\{^{11}B\})$ values as in each of these experiments the REDOR effect is diminished for the interaction between ^{23}Na and those ^{11}B nuclei, for which the recoupling pulse length chosen does not represent an effective π pulse. On the basis of this consideration, we consider the value of 49.8 × 10^6 rad^2 s^{-2} a lower limit; most likely $M_2(^{23}Na\{^{11}B\})$ is larger in this glass. (In the case of the borophosphate glasses, this issue is of no concern, as these glasses contain essentially only $B^{(4)}$ units, for which the π pulse length can be uniformly optimized.) Overall, the data in Table 5 show that the dipolar coupling between the ^{23}Na observe nuclei and the ^{11}B nuclei are significantly weaker in the borophosphate glasses than in $Na_2B_4O_7$ glass, indicating that the second coordination sphere of the sodium ions is not dominated by borate species. Of course, a reduced interaction is expected based on statistical considerations. Each of the 5−6 oxygen atoms within the first coordination sphere of a given sodium ion could be either linked to boron or to phosphorus, and if the second coordination spheres around the Na ions were arranged statistically, the $M_2(^{23}Na\{^{11}B\})$ values are expected to depend on the fractional contribution of the boron atoms to the network. Assuming that the Na---B distances in sodium borate and sodium borophosphate glasses are the same, one would therefore expect the $M_2(^{23}Na\{^{11}B\})$ value for glasses A, B, and C to be 1/5 (20%), 1/3 (33.3%), and

DOI: 10.1021/acs.jpcc.5b11608
J. Phys. Chem. C 2016, 120, 3196−3205

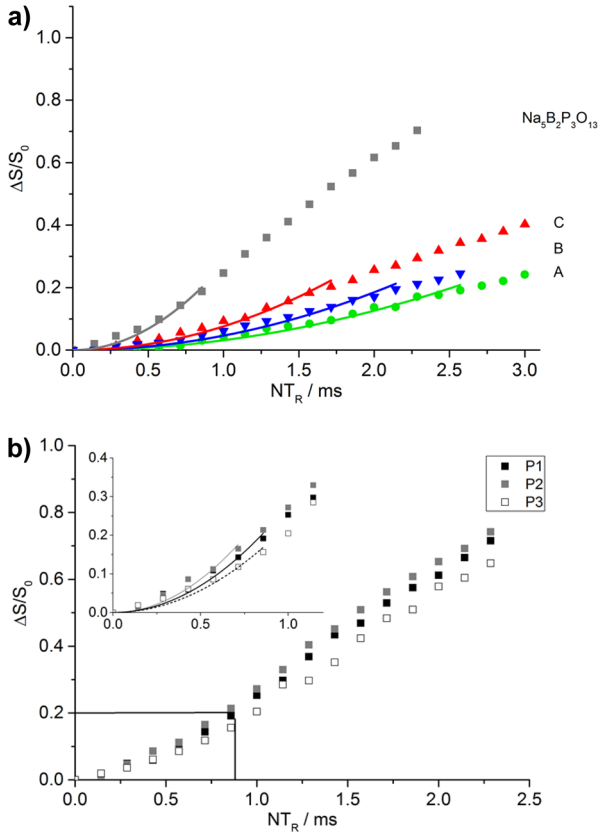

Figure 8. (a) $^{31}P\{^{23}Na\}$ REDOR results on samples A–C and on the model compound $Na_5B_2P_3O_{13}$. Measurement errors are represented by symbol sizes. For the model compound the average dephasing over the three spectroscopically resolved sites is presented. Parabolic fits (solid curves) were conducted within the range $\Delta S/S_0 < 0.2$. (b) $^{31}P\{^{23}Na\}$ REDOR results for the three crystallographically distinct phosphorus sites measured in the model compound $Na_5B_2P_3O_{13}$. Measurement errors are represented by symbol sizes. The inset shows a parabolic fit within the data range $\Delta S/S_0 \leq 0.2$.

1/4 (25%) of the respective value found in sodium diborate glass. The experimental values listed in Table 5 indicate that these values are significantly lower: they correspond to 12%, 29%, and 18%. Most likely these fractions are even smaller as the reference value of 49.8×10^6 rad^2 s^{-2} for sodium diborate glass is already an underestimate as outlined above. This diminution, which clearly reflects longer average Na---B distances (and/or under-representation of boron in the second coordination sphere of Na) in these borophosphate glasses, qualitatively supports the result from $^{23}Na\{^{31}P\}$ REDOR, pointing toward dominating Na—phosphate interactions. However, owing to the uncertainties in deriving accurate M_2 values from the parabolic fits in Figure 7, further evidence for this hypothesis is required. As discussed below, the most convincing evidence comes from a comparison of the $M_2(^{31}P\{^{23}Na\})$ and $M_2(^{11}B\{^{23}Na\})$ values.

$^{31}P\{^{23}Na\}$ and $^{11}B\{^{23}Na\}$ REDOR. The most definitive information regarding the cation–anion interactions in these borophosphate glasses comes from a comparison of the second moments $M_2(^{31}P\{^{23}Na\})$ and $M_2(^{11}B\{^{23}Na\})$ as determined from the corresponding REDOR experiments. Figures 8 and 9 summarize the experimental data on the glassy samples and the model compound $Na_5B_2P_3O_{13}$. The calibration factor f is measured by comparing the experimental M_2 values from the parabolic fit with the theoretical M_2 values calculated via equ. 1 from the crystal structure of $Na_5B_2P_3O_{13}$. Table 6 summarizes the experimental results on this model compound, carrying out the parabolic analysis over the initial data range. In the case of $^{31}P\{^{23}Na\}$ REDOR, excellent parabolic fits could be obtained over the data range $\Delta S/S_0 \leq 0.2$, resulting in three distinct values for the three spectroscopically resolved crystallographic phosphorus sites. The average calibration factor obtained from these measurements is 0.24. In the case of $^{11}B\{^{23}Na\}$ REDOR, the chemical shift difference between the two crystallographically distinct boron sites is too small to permit the measurement of separate M_2 values. Because the initial REDOR curvatures reveal substantial deviations from parabolic behavior at short evolution times, both for the model compound and for the glasses, the data range for the parabolic analysis was reduced to $\Delta S/S_0 \leq 0.1$ in this case, producing a calibration factor of 0.29. (As detailed in the Supporting Materials Section, however, the conclusions of the study remain the same, if we work with the poorer-quality fits obtained when the data analysis range is kept at $\Delta S/S_0 \leq 0.2$; in this case the calibration factor is 0.26).

Table 7 lists the experimental M_2 values and the corresponding values of $\sum r_{IS}^{-6}$ calculated from eq 1 for the three glasses studied, reflecting the effect of the distributions of the ^{23}Na nuclei about the ^{31}P and ^{11}B-observe nuclei. The quantity $\sum r_{IS}^{-6}$ allows a direct comparison of the data obtained from both $^{31}P\{^{23}Na\}$ REDOR and $^{11}B\{^{23}Na\}$ REDOR, as no nucleus-specific constants contribute to this quantity. Table 7 indicates that for all three glasses the values of $\sum r_{IS}^{-6}$ relating to the B–Na distance distributions ($\sum r_{B-Na}^{-6}$) are significantly

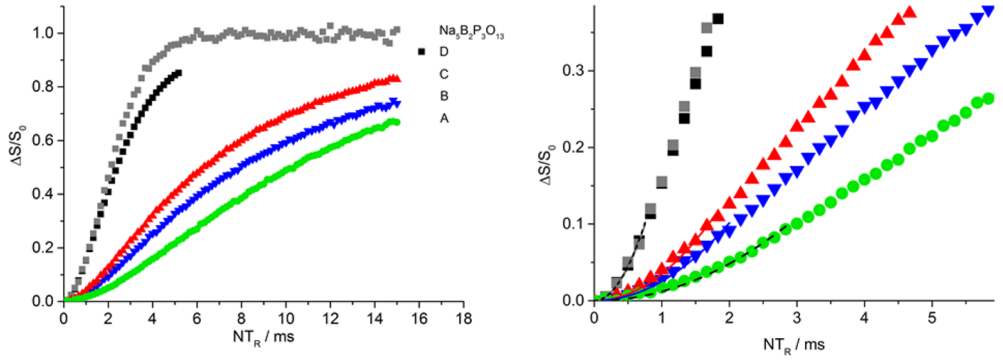

Figure 9. (left) $^{11}B\{^{23}Na\}$ REDOR results obtained for the glasses and $Na_5B_2P_3O_{13}$ and (right) parabolic fits (solid curves) to the data within the range $\Delta S/S_0 \leq 0.1$. Measurement errors are represented by symbol sizes.

DOI: 10.1021/acs.jpcc.5b11608
J. Phys. Chem. C 2016, 120, 3196–3205

Table 6. Second Moments $M_2/10^6$ s^{-2} (±10%) and Distance Sums $\sum r_{P-Na}^{-6}$ and $\sum r_{B-Na}^{-6}$ (±10%) Characterizing Heteronuclear Dipolar Interactions Determined from the $^{31}P\{^{23}Na\}$ and $^{11}B\{^{23}Na\}$ REDOR Experiments for the Model Compound $Na_5B_2P_3O_{13}$ Compared with the Theoretical Values from the Crystal Structure

	M_2 $^{31}P\{^{23}Na\}$				M_2 $^{11}B\{^{23}Na\}$		
P-position	exp	norm	$\sum r_{P-Na}^{-6}$ (10^{60} m^{-6})	B-position	exp	norm	$\sum r_{B-Na}^{-6}$ (10^{60} m^{-6})
P1	10.3	44.0	0.0067	B1, B2	6.5	22.1	0.0054
P2	12.8	47.9	0.0073				
P3	8.5	34.7	0.0053				

Table 7. Second Moments $M_2/10^6$ s^{-2} (±10%) and Distance Sums $\sum r_{P-Na}^{-6}$ and $\sum r_{B-Na}^{-6}$ (±10%) Characterizing the Dipolar Interaction Measured for the Glasses A–D from the Corresponding $^{31}P\{^{23}Na\}$ and $^{11}B\{^{23}Na\}$REDOR Experiments

	M_2 $^{31}P\{^{23}Na\}$			M_2 $^{11}B\{^{23}Na\}$		
sample	exp	norm	$\sum r_{P-Na}^{-6}$ (10^{60} m^{-6})	exp	norm	$\sum r_{B-Na}^{-6}$ (10^{60} m^{-6})
A	1.2	4.9	0.0007	0.4	1.5	0.0004
B	1.7	7.1	0.0011	0.9	3.2	0.0008
C	2.8	11.7	0.0018	1.3	4.4	0.0011
D				6.7 ($B^{(4)}$)	22.6	0.0055
				6.7 ($B^{(3)}$)	22.6	0.0055

lower than the values of $\sum r_{IS}^{-6}$ relating to the P–Na distance distributions ($\sum r_{P-Na}^{-6}$). This result clearly indicates that the phosphate species are (on average) significantly closer to the sodium ions than the borate species, despite the low concentrations of anionic $P^{(2)}$ units in these glasses.

Table 7 indicates further that the $\sum r_{P-Na}^{-6}$ and $\sum r_{B-Na}^{-6}$ values for glasses A–C are different from each other and substantially lower than those measured for the model compound. This effect is expected based on the different concentrations of sodium ions (13.3, 25, and 33.3 mol % in glasses A, B, and C and 50 mol % in $Na_5B_2P_3O_{13}$). As discussed previously for binary sodium borate glasses in the limit of very low sodium concentrations, the $^{11}B\cdots^{23}Na$ dipolar interaction can be approximated by a two-spin interaction, and an internuclear distance of 316 pm was deduced from REDOR measurements.[34] We also showed previously that in sodium phosphate glasses with low sodium contents the $^{31}P\cdots^{23}Na$ dipolar couplings can be approximated by a two-spin interaction, with an internuclear distance of 330 pm as deduced from $^{31}P\{^{23}Na\}$ REDOR.[35] Owing to the statistical distribution of the network modifier ions in both binary glass systems, the strengths of the $^{11}B-^{23}Na$ and of the $^{31}P-^{23}Na$ dipole–dipole interactions (and hence the values of $\sum r_{IS}^{-6}$) are always expected to increase with increasing sodium concentration, as the distances between different spin pairs decrease and larger spin interaction clusters start to appear. Figure 10 compares these concentration dependences of $\sum r_{IS}^{-6}$ of the present borophosphate glasses with those calculated from previously published M_2 data of binary sodium borate[34] and binary sodium phosphate glasses.[35] Clearly, the values of $\sum r_{P-Na}^{-6}$ of the mixed-network former glasses are close to those of the sodium phosphate glasses having similar Na concentrations; as a matter of fact, they lie above those obtained for the $P^{(3)}$ groups and agree well with those obtained for the interactions between the anionic $P^{(2)}$ groups. In contrast, the $\sum r_{B-Na}^{-6}$ values in the borophosphate glasses are significantly lower than those measured in binary sodium borate glasses with comparable sodium concentrations. Once again, this result confirms that—despite their formally uncharged status—the $P^{(3)}$ phosphate groups are the chief charge-compensating species in our glasses. The negative formal charge located on the $B^{(4)}_{4P}$ units is actually not found there, but it is dispersed into the network owing to the bond valence gradient encountered in the B–O–P linkages. As predicted in ref 16, this mechanism leads to a redistribution of Coulomb traps, accounting for the increased ionic mobility observed.

CONCLUSIONS

Based on the dipolar analysis described above, the results of the present study show that the network modifier–network former interactions in sodium borophosphate glasses show much closer resemblance to the behavior of sodium phosphate rather than sodium borate networks. Thus, in glasses with high concentrations of B–O–P linkages the principal charge compensation of the Na^+ ions occurs via partial anionic charges

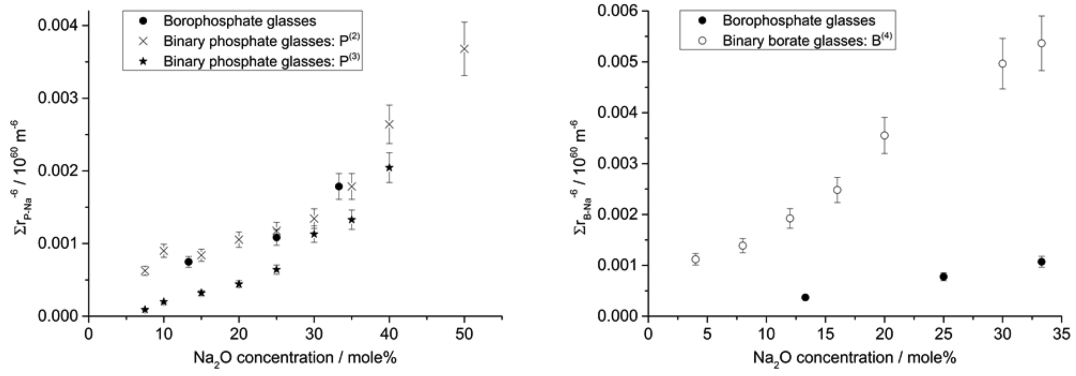

Figure 10. Dependence of the distance sums $\sum r_{B-Na}^{-6}$ and $\sum r_{P-Na}^{-6}$ on sodium ion concentration in binary sodium borate,[34] binary sodium phosphate,[35] and the sodium borophosphate glasses of the present study.

DOI: 10.1021/acs.jpcc.5b11608
J. Phys. Chem. C 2016, 120, 3196–3205

located on the phosphate rather than the borate species, even though the $B^{(4)}$ units are formally negatively charged. The charge dispersal mechanism illustrated in Figure 1 most likely results in shallower Coulomb traps, thereby facilitating ionic jumps between different sites. This charge dispersal mechanism afforded by a strong heteroatomic connectivity preference offers a new structural rationale for the positive mixed-network former effect observed in alkali borophosphate glasses.

■ ASSOCIATED CONTENT

Supporting Information

The Supporting Information is available free of charge on the ACS Publications website at DOI: 10.1021/acs.jpcc.5b11608.

Peak deconvolution of the ^{11}B MAS NMR spectra of Figure 3; alternative second moment analysis of the $^{11}B\{^{23}Na\}$ REDOR data based on the data range $\Delta S/S_0 \leq 0.2$ (PDF)

■ AUTHOR INFORMATION

Corresponding Author

*E-mail: eckerth@uni-muenster.de (H.E.).

Notes

The authors declare no competing financial interest.

■ ACKNOWLEDGMENTS

The authors acknowledge the Brazilian funding agency FAPESP (CEPID Project 2013/07793-6). L.F. thanks the Foundation of German Business and the Manfred-Lautenschläger Foundation for a personal stipend.

■ REFERENCES

(1) Levasseur, A.; Olazuaga, R.; Kbala, M.; Zahir, M.; Hagenmuller, P.; Couzi, M. Etudes Electrique et Raman des Verres des Systemes B_2O_3-M_2O-M_3PO_4 (M = Li, Na). *Solid State Ionics* **1981**, *2*, 205−213.

(2) Salodkar, R. V.; Deshpande, J. K.; Singh, K. Enhancement of the Ionic Conductivity In Lithium Borophosphate Glass: A Mixed Glass-former Approach. *J. Power Sources* **1989**, *25*, 257−263.

(3) Takebe, H.; Harada, T.; Kuwabara, M. Effect of B_2O_3 Addition on the Thermal Properties and the Densities of Barium Phosphate Glasses. *J. Non-Cryst. Solids* **2006**, *352*, 709−713.

(4) Christensen, R.; Olson, G.; Martin, S. W. Ionic Conductivity of Mixed Glass Former 0.35 Na_2O + 0.65[xB_2O_3 + (1-x)P_2O_5] Glasses. *J. Phys. Chem. B* **2013**, *117*, 16577−16586.

(5) Videau, J. J.; Ducel, J. F.; Suh, K. S.; Senegas, J. P-31 MAS and B-11 NMR Study of Sodium-Rich Borophosphate Glasses. *Phys. Chem. Glasses* **1994**, *35*, 10−16.

(6) Ducel, J. F.; Videau, J. J. Physical and Chemical Characterization of Sodium Borophosphate Glasses. *Mater. Lett.* **1992**, *13*, 271−274.

(7) Zielniok, D.; Cramer, C.; Eckert, H. Structure/Property Correlations in Ion-Conducting Mixed-Network Former Glasses: Solid State NMR Studies of the System Na_2O-B_2O_3-P_2O_5. *Chem. Mater.* **2007**, *19*, 3162−3170.

(8) Christensen, R.; Olson, G.; Martin, S. W. Structural Studies of Mixed Glass Former 0.35Na_2O + 0.65[xB_2O_3 + (1-x)P_2O_5] Glasses by Raman and ^{11}B and ^{31}P Magic Angle Spinning Nuclear Magnetic Resonance Spectroscopies. *J. Phys. Chem. B* **2013**, *117*, 2169−2176.

(9) Larink, D.; Eckert, H.; Reichert, M.; Martin, S. W. The Mixed Network Former Effect in Ion-Conducting Alkali Borophosphate Glasses: Structure/Property Correlations in the System $[M_2O]_{1/3}[(B_2O_3)_x(P_2O_5)_{1-x}]_{2/3}$ (M = Li, K, Cs). *J. Phys. Chem. C* **2012**, *116*, 26162−26176.

(10) Raskar, D.; Rinke, M. T.; Eckert, H. The Mixed-Network Former Effect in Phosphate Glasses: XPS and NMR Studies of the Connectivity Distribution in the Glass System $(NaPO_3)_{1-x}(B_2O_3)_x$. *J. Phys. Chem. C* **2008**, *112*, 12530−12539.

(11) Rinke, M. T.; Eckert, H. The Mixed Network Former Effect in Glasses: Solid State NMR and XPS Structural Studies of the Glass System $(Na_2O)_x(BPO_4)_{1-x}$. *Phys. Chem. Chem. Phys.* **2011**, *13*, 6552−6565.

(12) Raguenet, B.; Tricot, G.; Silly, G.; Ribes, M.; Pradel, A. Revisiting the "Mixed Network Former Glass Effect" in Ultrafast-Quenched Borophosphate Glasses by Advanced 1D/2D NMR Methods. *J. Mater. Chem.* **2011**, *21*, 17693−17704.

(13) Raguenet, B.; Tricot, G.; Silly, G.; Ribes, M.; Pradel, A. The Mixed Glass Former Effect in Twin-roller Quenched Lithium Borophosphate Glasses. *Solid State Ionics* **2012**, *208*, 25−30.

(14) Tricot, G.; Raguenet, B.; Silly, G.; Ribes, M.; Pradel, A.; Eckert, H. First Evidence of P-O-B^{III} Linkage in Alkali and Silver Borophosphate Glasses by High Field Correlation NMR. *Chem. Commun.* **2015**, *51*, 9284−9286.

(15) Schuch, M.; Christensen, R.; Trott, C.; Maass, P.; Martin, S. W. Investigation of the Structure of Sodium Borophosphate Glasses by Reverse Monte Carlo Modelling to Explain the Origin of the Mixed Glass Former Effect. *J. Phys. Chem. C* **2012**, *116*, 1503−1511.

(16) Schuch, M.; Trott, C.; Maass, P. Network Forming Units in Alkali Borate and Borophosphate Glasses and the Mixed Glass Former Effect. *RSC Adv.* **2011**, *1*, 1370−1382.

(17) Tho, T. D.; Rao, R. P.; Adams, S. Structure Property Correlation in Lithium Borophosphate Glasses. *Eur. Phys. J. E: Soft Matter Biol. Phys.* **2012**, *35* (8), 1−11.

(18) van Vleck, J. H. The Dipolar Broadening of Magnetic Resonance Lines in Crystals. *Phys. Rev.* **1948**, *74*, 1168−1183.

(19) Gullion, T.; Schaefer, J. Rotational Echo Double Resonance NMR. *J. Magn. Reson.* **1989**, *81*, 196−200.

(20) Medek, A.; Harwood, J. S.; Frydman, L. Multiple-Quantum Magic-Angle Spinning NMR: A New Method for the Study of Quadrupolar Nuclei in Solids. *J. Am. Chem. Soc.* **1995**, *117*, 12779−12787.

(21) Medek, A.; Frydman, L. Multiple-Quantum Magic-Angle Spinning NMR: A New Technique for Probing Quadrupolar Nuclei in Solids. *J. Braz. Chem. Soc.* **1999**, *10*, 263−277.

(22) Massiot, D.; Fayon, F.; Capron, M.; King, I.; Calve, S. L.; Alonso, B.; Durand, J. O.; Bujoli, B.; Gan, Z.; Hoatson, G. Modelling One- and Two-Dimensional Solid-State NMR Spectra. *Magn. Reson. Chem.* **2002**, *40*, 70−76.

(23) Hauf, C.; Friedrich, T.; Kniep, R. Crystal Structure of Pentasodium catena-(diborato-triphosphate), $Na_5[B_2P_3O_{13}]$. *Z. Kristallogr. - Cryst. Mater.* **1985**, *210*, 446−446.

(24) Garbow, J. R.; Gullion, T. Improvements in REDOR NMR Spectroscopy. Minimizing Resonance-offset Effects. *J. Magn. Reson.* **1991**, *95*, 442−445.

(25) Bertmer, M.; Eckert, H. Dephasing of Spin Echoes by Multiple Dipolar Interactions in Rotational Echo Double Resonance NMR Experiments. *Solid State Nucl. Magn. Reson.* **1999**, *15*, 139−152.

(26) Strojek, W.; Kalwei, M.; Eckert, H. Dipolar NMR Strategies for Multispin Systems Involving Quadrupolar Nuclei: ^{31}P ^{23}Na Rotational Echo Double Resonance (REDOR) of Crystalline Sodium Phosphates and Phosphate Glasses. *J. Phys. Chem. B* **2004**, *108*, 7061−7073.

(27) Chan, J. C. C.; Bertmer, M.; Eckert, H. Site Connectivities in Amorphous Materials Studied by Double Resonance NMR of Quadrupolar Nuclei: High Resolution $^{11}B \leftrightarrow {}^{27}Al$ Spectroscopy of Aluminoborate Glasses. *J. Am. Chem. Soc.* **1999**, *121*, 5238−5248.

(28) Strojek, W.; Fehse, C. M.; Eckert, H.; Ewald, B.; Kniep, R. Site Discrimination in the Crystalline Borophosphate $Na_5B_2P_3O_{13}$ Using Solid-State NMR Techniques. *Solid State Nucl. Magn. Reson.* **2007**, *32*, 89−98.

(29) Hudgens, J. J.; Brow, R. K.; Tallant, D. R.; Martin, S. W. Raman Spectroscopy Study of the Structure of Lithium and Sodium Ultraphosphate Glass. *J. Non-Cryst. Solids* **1998**, *223*, 21−31.

(30) Konijendijk, W. L.; Stevels, J. M. Structure of Borate Glasses Studied by Raman Scattering. *J. Non-Cryst. Solids* **1975**, *18*, 307−331.

(31) Bril, T. W. Raman Spectroscopy of Crystalline and Glassy Borates. *Phillips Res. Rep. Suppl.* **1976**, *2*, 1−114.

DOI: 10.1021/acs.jpcc.5b11608
J. Phys. Chem. C 2016, 120, 3196−3205

(32) Dwivedi, B. P.; Khanna, B. N. Cation Dependence of Raman Scattering in Alkali Borate Glasses. *J. Phys. Chem. Solids* **1995**, *56*, 39−49.
(33) Hidi, I. J.; Melinte, G.; Stefan, R.; Bindea, M.; Baia, L. The Structure and Bioactivity of the Na_2O-B_2O_3-P_2O_5 System. *J. Raman Spectrosc.* **2013**, *44*, 1187−1194.
(34) Epping, J. D.; Strojek, W.; Eckert, H. Cation Environments and Spatial Distribution in Na_2O-B_2O_3 Glasses: New Results from Solid State NMR. *Phys. Chem. Chem. Phys.* **2005**, *7*, 2384−2389.
(35) Strojek, W.; Eckert, H. Medium-range Order in Sodium Phosphate Glasses: A Quantitative Rotational Echo Double Resonance Solid State NMR Study. *Phys. Chem. Chem. Phys.* **2006**, *8*, 2276−2285.

DOI: 10.1021/acs.jpcc.5b11608
J. Phys. Chem. C 2016, 120, 3196−3205